

The XIII International Conference on the Physics of Non-Crystalline

Solids

Correlation between Hydrophilicity and Surface Aggregation in Anodized TiO₂ Nanotube Arrays

Wenjuan Yang¹, Qi Peng², Rong Chen², Yanwei Wen^{1*}, Bin Shan¹

¹State Key Laboratory of Material Processing and Die and Mould Technology and School of Materials Science and Engineering, Huazhong University of Science and Technology, Wuhan (430074), Hubei, China

²State Key Laboratory of Digital Manufacturing Equipment and Technology and School of Mechanical Science and Engineering, Huazhong University of Science and Technology, Wuhan (430074), Hubei, China

Abstract

Aligned TiO₂ nanotube array through anodization method often comes with a surface aggregation layer of TiO₂ nanowires. To achieve high photoelectrochemical(PEC) performance, aggregation must be avoided during synthesis or removed via post-processing methods. We present here an efficient method of evaluating the extent of surface aggregation on TiO₂ nanotube arrays through water contact angle measurement. Our results indicate that water contact angle on a clean TiO₂ nanotube array is almost negligible, with a good correlation between aggregate coverage ratio and contact angles as the aggregation layer increases. This enables a convenient and reliable procedure for quantitatively characterize the surface aggregate level on a macroscopic scale.

© 2013 The Authors. Published by Elsevier B.V.

Selection and peer-review under responsibility of Prof. Xiujian Zhao, Wuhan University of Technology

* Corresponding author. Tel: 86-27-87559843. E-mail address: ywwen@mail.hust.edu.cn

Keywords: TiO₂ Nanotube, Aggregation, Water Contact Angle

1. Introduction

Ordered TiO₂ nanotube arrays (NTAs) with high surface-to-volume ratio possess outstanding properties like superior charge transportation, making them suitable candidates for a variety of advanced applications such as hydrogen generation from water splitting[1], dye-sensitized solar cell[2-6], gas sensor[7], and biomedicine[8]. In recent years, there have been many reports on the synthesis strategies of nanotubular TiO₂ film structures, such as template-based method[9], hydrothermal process[10] and anodic oxidation of titanium[11, 12]. Among these methods, anodic oxidation is one of the most widely used methods to synthesize nanotube TiO₂ as its dimensions can be precisely controlled. However, one of the challenges is to remove the surface aggregation covering the NTAs' surface which frequently forms during the synthesis process. Lim and Choi [13] have built a "bamboo splitting" model to explain the reason of aggregation formation. They pointed out that in high potential, the electrolysis occurs not only at the tip but also on the whole surface of NTAs, and the result of coverage on the surface will induce stress among tubes, thus impelling the production of the nanowires. Zhu et al. [14] suggested two ways of producing pure TiO₂ without aggregation. One is to directly fabricate pure TiO₂ in secondary reaction electrolyte of NH₄F and H₂O in ethylene glycol; the other is to remove aggregation by ultrasonic cleaning in ethyl alcohol and then rinsing in double distilled water. The experimental condition of ultrasonic method have been intensively studied to remove the aggregation[15]. Moreover, other method like forming a protected layer on TiO₂ NTAs has also been tried to prevent the aggregation and avoid the tube corrosion[16]. Removing aggregation is essential for improving sunlight absorbing capability, enhancing ionic diffusion through the channels and charge transportation along the tube.

To ensure complete removal of surface aggregation, SEM analysis is widely used to characterize the surface morphology of TiO₂ NTAs. However, it is destructive to the sample and only probes a local area. Herein, we present an alternative and efficient method that complements the traditional SEM analysis. We utilize the water contact angle to evaluate the extent of surface aggregation of TiO₂ NTAs. Our results show that aggregation is composed of TiO₂ nanowires and ultrasonic in water is an effective way of removing it. Also, water contact angle shows good correlation to the extent of aggregation on the NTA surface.

2 Experiments

2.1. Fabrication of TiO₂ NTAs

Pure titanium foil (thickness is about 0.5 mm and purity >99%) with working area reaching 1.0 cm² -7.0 cm² is firstly polished with a silicon carbide paper (from 400 to 1200 grade), then rinsed with acetone, and finally rinsed with deionized (DI) water. The anodization is performed using a two-electrode cell, in which titanium foil is used as the working electrode and Pt as the counter electrode with a distance of 3 cm at room temperature (approximately 28 °C). The titanium foil is immersed in a solution of 0.3wt% NH₄F and 3vol% H₂O in ethylene glycol for 10 h at the voltage of 58 V. Afterwards, the samples are immersed in ethanol for 30min, dried in an oven at 100 °C, and then ultrasonic cleaned in DI water. At last, the samples are annealed at 300 °C for 2h with a heating and cooling rate of 2 °C/min.

2.2. Removal of surface aggregation by sonication

In the process of sonication, Ti is hung up in the solution of water instead of leaving in the beaker in order to avoid breaking NTAs into pieces. 40 KHz is found to be a suitable frequency as higher frequencies may do

damage to the NTAs. 5-10 min is a balancing point at which aggregation is removed while NTAs keeps its geometrical features.

2.3. Contact angle and PEC test

Contact angle measurement is conducted at a temperature of 22°C with a commercial contact angle analyzer (USA Kino Industry Co., Ltd). The droplet amount used for the measurements is 2 μ L. Water droplets are placed at five different positions on each sample and the average value is adopted as the contact angle.

Photoelectrochemical (PEC) performance measurement is conducted by using TiO₂ nanotube photoanode as the working electrode, Pt foil as counter electrode, and Ag/AgCl as reference electrode. The solution in PEC is 1 M Na₂S, which is an electron capturer. Voltage and current are recorded by a computer controlled electrochemical analyzer (Correst 310). The simulated sunlight is from a full-spectrum 500 W Solar Simulator (CHF-XM500, Trusttech), with an illumination intensity of 100 mW/cm² as measured by a Solar Power Detector (TES 1333). The photocurrent voltage range is -1.2~1.5 V (versus Ag/AgCl) with a rate of 10mV/s under illumination. Photoconversion efficiency of light energy to chemical energy in the presence of an external applied potential is calculated using the following expression:

$$\eta(\%) = j_p \left[(E_{\text{rev}}^0 - |E_{\text{app}}|) / I_0 \right] \times 100 (\%) \quad (1)$$

where E_{rev}^0 equals 1.23 V and represents the potential corresponding to the Gibbs free energy change per photon in the water splitting reaction. $E_{\text{app}} = E_{\text{means}} - E_{\text{aoc}}$, where the term E_{means} is the electrode potential (vs. Ag/AgCl) of the working electrode and E_{aoc} is the electrode potential (vs. Ag/AgCl) of the same working electrode at open-circuit condition under same illumination and in the same electrolyte solution. j_p is the photocurrent density, and I_0 is the intensity of incident light.

3 Results & Discussion

3.1. Surface characterization of the synthesized TiO₂ NTAs by SEM

Fig. 1 shows SEM images of the TiO₂ NTAs sample grown from a 0.3% NH₄F + 3vol% H₂O in ethylene glycol for 10 h at 58 V. Among all the images, Fig. 1a-b show the morphology of TiO₂ before ultrasonic treatment, while Fig. 1c (low magnification) and its inset (high magnification) are those of TiO₂ after ultrasonic treatment. As can be seen from Fig. 1a, the whole length of the tube is about 40 μ m, with nanotubes splitting into nanowires at tip regions (~ 5 μ m). On the top surface, the nanowires twine together, resulting in the aggregation layer clogging the holes of NTAs (Fig. 1b). Due to the existence of the surface aggregation layer, the photocatalytic performance may be degraded owing to less reactant into large inner pores. In order to improve photocatalytic performance, finding an efficient way to characterize and remove aggregation is of great practical importance. Ultrasonic cleaning is believed to be one of the effective ways to get ordered TiO₂ NTAs. In the process of ultrasonic treatment, some white sediment can be observed to drop out from TiO₂ nanotubes array, indicating that breakdown and removal of aggregates. The nanotubes obtained from ultrasonic treatment with standard processing time do not suffer from aggregation, and present open and unclogged pores with a diameter of 100 nm and a wall thickness of about 20-30nm, as shown in Fig.1c and Fig.1d.

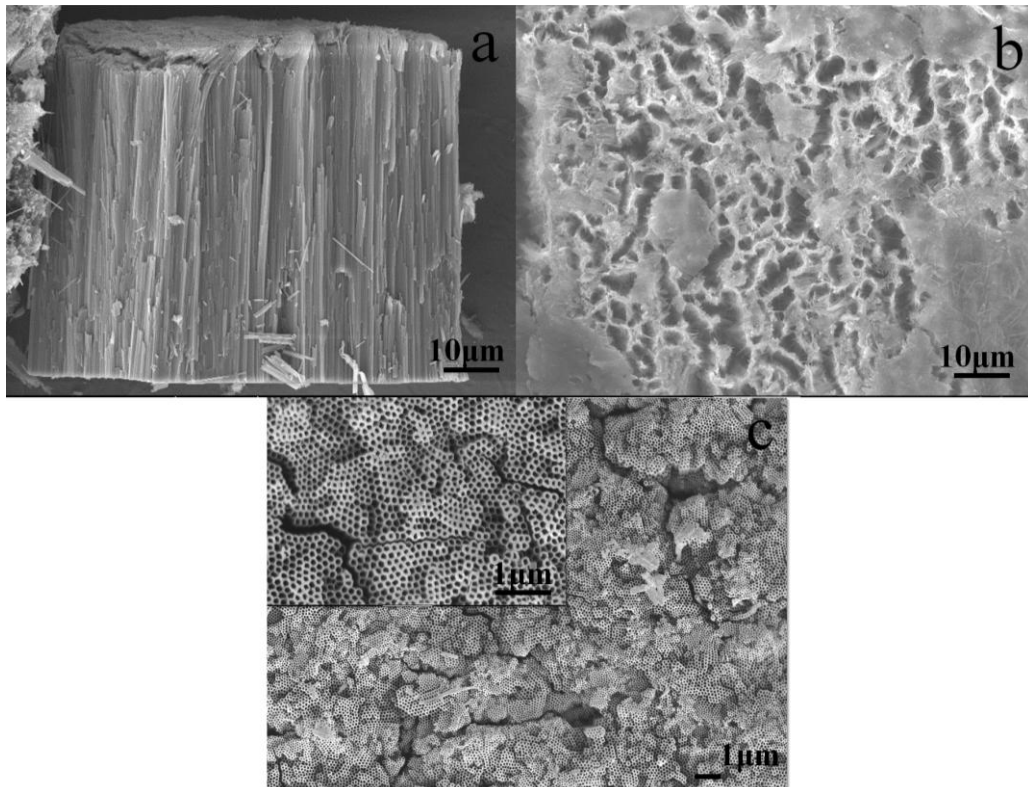


Fig. 1. FE-SEM images of a TiO_2 NTAs sample grown from a 0.3% NH_4F + 3vol% H_2O in ethylene glycol for 10 h at 58 V before ultrasonic: (a) side-view image, (b) top-view image, (c) SEM image with an inset after ultrasonic for 5 min.

3.2. Surface characterization of the synthesized TiO_2 NTAs by water contact angle

As displayed in Fig. 2a-c, aggregations are rapidly decreasing under ultrasonic treatment at different stages, ranging from large area of nanowires covering the surface to partly covered surface, and then to a clean surface. After analyzing the SEM images (using software Image J), we estimate that the coverage ratio f is 100%, 42%, 0 for Fig. 2a, Fig. 2b and Fig. 2c, respectively. While the corresponding the measured contact angles images are shown in their insets. The water contact angle gradually decreases from 40° to 32° as shown in insets of Fig. 2a and Fig. 2b. On a clean TiO_2 NTA surface, the contact angle is close to 0° and the $2\mu\text{L}$ water spreads and permeates instantly (around 0.5s) when dropped onto the surface, indicating the superhydrophilic nature of the clean surface (inset of Fig. 2c). Therefore, we conclude that there exists a correlation between the aggregation coverage ratio and the water contact angle. The relationship is shown in Fig. 2d. From the figure, water contact angle is not sensitive to coverage when it is below the critical angle θ_0 ($\theta_0=24^\circ$), in part due to the intrinsic limitation of water contact measurement at low angles. Nevertheless, with surface aggregation increases, the water contact angle show appreciable change from 24° to 40° , and roughly in a linear proportion. Equation (2) empirically fits the relationship between contact angle and coverage ratio

$$f \propto k \times (\theta - \theta_0) \quad (2)$$

where f , θ and k are coverage ratio, contact angle and coefficient ratio, respectively. It should be noticed that the aggregate coverage ratio on NTA surface is gradually decreasing with the increase of ultrasonic time at the first 5 minutes in our experiment. Beyond this time, the aggregation on the NTA surface is totally removed and coverage ratio measured by water contact angle is nearly zero, that is, ultrasonic time would not affect aggregate coverage ratio after that time. However, too much ultrasonic time may destroy the TiO₂ nanotubes into pieces.

According to the coverage ratio based on the SEM characterizations, k is estimated to be 5.86 with an error bar of 0.6. This indicates that a larger water contact angle corresponds to more severe aggregation in an appropriate sense, serving as an efficient, non-destructive way of characterizing surface aggregation in TiO₂ NTAs.

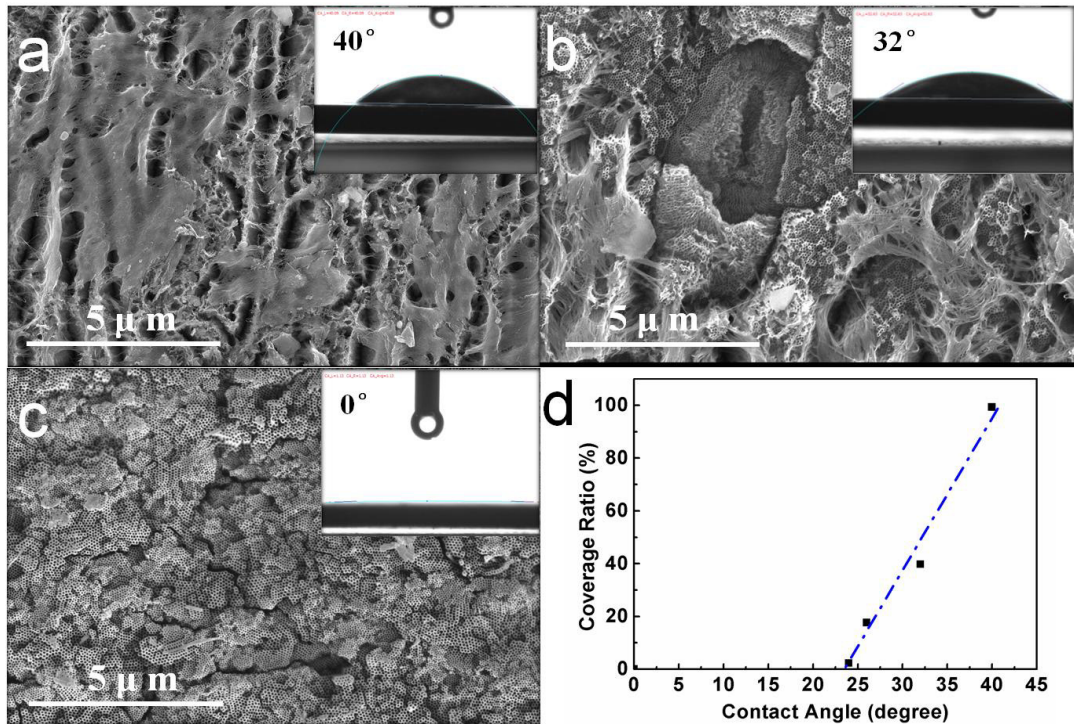


Fig. 2. (a), (b) and (c) are SEM images of the synthesized TiO₂ with different ultrasonic treatment time, the insets show corresponding contact angles measurement. (d) indicates the relationship between contact angle and coverage ratio of TiO₂ NTAs.

3.3. Water contact angle model

The trend of the water contact angle change as a function of surface coverage can be rationalized within the framework of Wenzel's theory (formula 3):

$$\cos \theta = r \cos \theta_0 \quad (3)$$

Where θ_0 is the contact angle for smooth surface and r is a roughness factor defined as a ratio of an actual

rough surface area to the geometrically projected area. Assuming that the actual solid area equals the sum of the geometrically projected area (S_p) and the total surface area of the side-walls (S_w), the roughness factor r can be estimated by $r=(S_p+ S_w)/S_p$. In our case, S_p is the given area for each SEM image of surface morphology, and S_w approximately equals to the sum of interior and exterior specific area which can be calculated from Fig. 1. For our NTAs, the surface roughness r is calculated to range from 10 to 700, and the cosine of water contact angle ($\cos\theta$) is in proportion to roughness r .

It should be mentioned that opposite results have been previously reported for anodic aluminum oxide (AAO)[17]. The reason lies primarily in the different nature of the surface aggregation: for AAO, the nanowires dissolved by electrolyte are standing up on the surface and enlarge the diameter of the AAO pores, thus making water infuse into the pores easily. Thus the surface layer has increased S_w . In contrast, for NTAs, the aggregation lying on surface blocks that water permeation, thus effectively diminish the area of side walls S_w . Since the roughness is equal to $r_0 \times f_{\text{coverage}}$ (r_0 means roughness of TiO_2 NTAs with clean surface), the enhancement of f_{coverage} gives rise to the reduction of the roughness (shown as Fig. 3b). It can be concluded that the morphology plays an important role in determining the differences of contact angle behavior between AAO and TiO_2 NTAs.

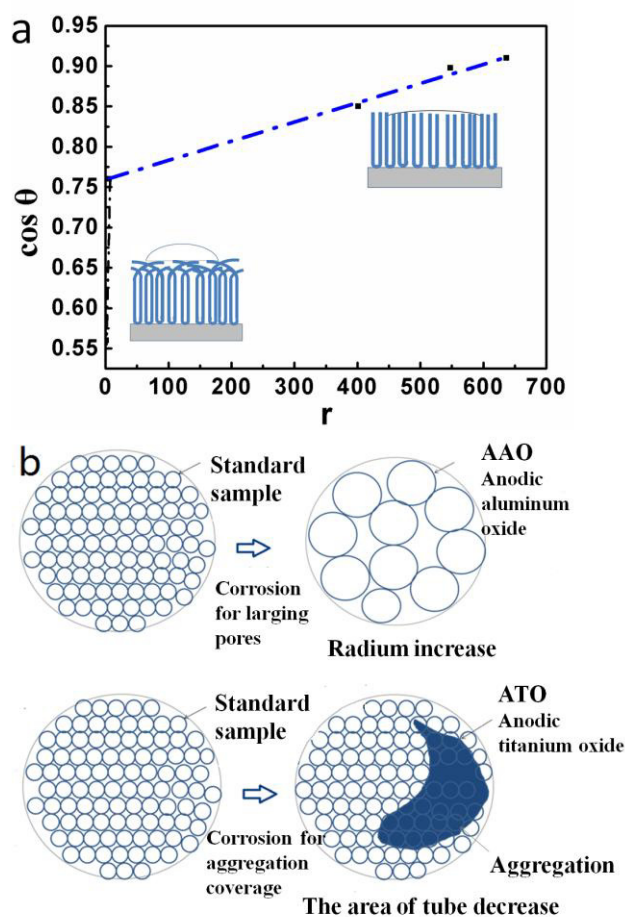


Fig.3. (a) water contact angles as a function of surface roughness factor for TiO_2 . (b) Schematic diagram on the roughness factor impacting on the AAO and NTAs

4. PEC performance

After removing aggregation from the surface, the photocurrent performance can be enhanced as evidenced by amplified photocurrent. Fig.4. shows the relationship between coverage ratio and photoconversion efficiency. When the water contact angle diminishes, photoconversion efficiency increases correspondingly. The PEC can reach 1.48% when aggregation layer is removed from the NTA surface. The reason for the photocatalytic performance improvement can be attributed to the removal of structural disorder from oriented TiO₂ NTAs and the corresponding reduction in the dimensionality of transport and recombination rates of electron and holes[18]. It is clear that a smooth surface morphology without surface aggregation shows better PEC performance.

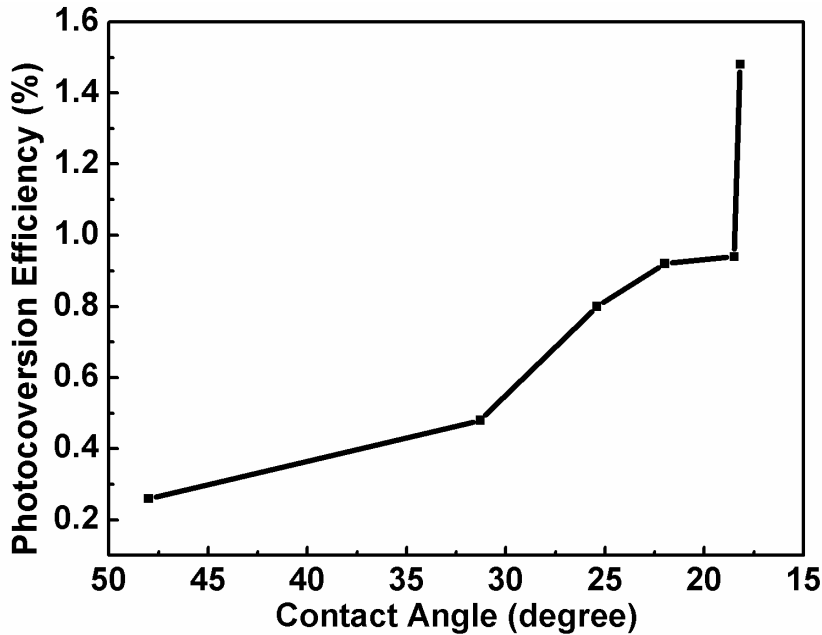


Fig. 4. Relationship between contact angle and photoconversion efficiency

5. Conclusions

We established a correlation between water contact angle and aggregate coverage ratio on NTA surface, enabling a convenient and reliable screening procedure for the confirmation of surface aggregate removal on the macroscopic scale. The reason for water contact angle change can be explained by Wenzel's theory. Our results show improved PEC performance after the removal of the aggregates on the surface.

Acknowledgements

This work is supported National Natural Science Foundation of China (Grant 11004068 and 51101064) and Fundamental Research Funds for the Central Universities, HUST (2012TS012 and 2012TS076). The authors acknowledge the Thousand Young Talents Plan and New Century Excellent Talents in University (NCET).

References

- [1] Fujishima. A, Honda. K., 1972. Electrochemical Photolysis of Water at a Semiconductor Electrode. *Nature*. 238, p. 37.
- [2] Gratzel M., 2001. Photoelectrochemical cells. *Nature*. 414, p. 338-44.
- [3] O'Regan B, Gratzel M., 1991. A low-cost, high-efficiency solar cell based on dye-sensitized colloidal TiO₂ films. *Nature*. 353, p. 737.
- [4] Varghese OK, Paulose M, Grimes CA., 2009. Long vertically aligned titania nanotubes on transparent conducting oxide for highly efficient solar cells. *Nature. Nanotechnology*. 4, p. 4592.
- [5] Wang H, Yip CT, Cheung KY, Djuricic AB, Xie MH, Leung YH, Chan WK., 2006. Titania-nanotube-array-based photovoltaic cells. *Apply. Physic. Letter*. 89, p. 023508.
- [6] Xu C, Shin PH, Cao L, Wu J, Gao D., 2009. Ordered TiO₂ Nanotube Arrays on Transparent Conductive Oxide for Dye-Sensitized Solar Cells. *Chemical. Material*. 22, p. 143.
- [7] Seo M-H, Yuasa M, Kida T, Huh J-S, Shimano K, Yamazoe N., 2009. Gas sensing characteristics and porosity control of nanostructured films composed of TiO₂ nanotubes. *Sensors Actuators. B-Chemical*. 137, p. 513.
- [8] Yang B, Uchida M, Kim HM, Zhang X, Kokubo T., 2004. Preparation of bioactive titanium metal via anodic oxidation treatment. *Biomaterials*. 25, p. 1003.
- [9] Hoyer P., 1996. Formation of a Titanium Dioxide Nanotube Array. *Langmuir*. 12, p. 1411.
- [10] Chen Q, Zhou W, Du GH, Peng LM., 2002. Trititanate Nanotubes Made via a Single Alkali Treatment. *Advance. Material*. 14, p. 1208.
- [11] Cai Q, Paulose M, Varghese OK, Grimes CA., 2005. The Effect of Electrolyte Composition on the Fabrication of Self-Organized Titanium Oxide Nanotube Arrays by Anodic Oxidation. *Journey of Materials Research*. 20, p. 230.
- [12] Macak JM, Tsuchiya H, Taveira L, Aldabergerova S, Schmuki P., 2005. Smooth Anodic TiO₂ Nanotubes. *Angewandte Chemie International Edition*; 44, p. 7463.
- [13] Lim JH, Choi J., 2007. Titanium Oxide Nanowires Originating from Anodically Grown Nanotubes: The Bamboo-Splitting Model. *Small*. 3, p. 1504.
- [14] Zhu W, Liu X, Liu H, Tong D, Yang J, Peng J., 2010. Coaxial Heterogeneous Structure of TiO₂ Nanotube Arrays with CdS as a Superthin Coating Synthesized via Modified Electrochemical Atomic Layer Deposition. *Journey of America Chemical Society*. 132, p. 12619.
- [15] Xu H, Zhang Q, Zheng C, Yan W, Chu W., 2011. Application of ultrasonic wave to clean the surface of the TiO₂ nanotubes prepared by the electrochemical anodization. *Apply. Surface. Science*. 257, p. 8478.
- [16] Song Y-Y, Lynch R, Kim D, Roy P, Schmuki P., 2009. TiO₂ Nanotubes: Efficient Suppression of Top Etching during Anodic Growth. *Electrochemical and Solid State Letters*. 12, p. C17.
- [17] Ye J, Yin Q, Zhou Y., 2009. Superhydrophilicity of anodic aluminum oxide films: From honeycomb to bird's nest *Thin Solid Films*. 517, p. 6012.
- [18] Zhu K, Vinzant TB, Neale NR, Frank AJ., 2007. Removing Structural Disorder from Oriented TiO₂ Nanotube Arrays: Reducing the Dimensionality of Transport and Recombination in Dye-Sensitized Solar Cells. *Nano Letter*. 7, p. 3739.